Temporal and Spatial Dynamics of Estuarine Shoreline Change in the Albemarle-Pamlico Estuarine System, North Carolina, USA

Devon O. Eulie [1,2,5] · J. P. Walsh [1,2,3] · D. Reide Corbett [1,2,3] · Ryan P. Mulligan [4]

Abstract Many shoreline studies rely on historical change rates determined from aerial imagery decades to over 50 years apart to predict shoreline position and determine setback distances for coastal structures. These studies may not illustrate the coastal impacts of short-duration but potentially high-impact storm events. In this study, shoreline change rates (SCRs) are quantified at five different sites ranging from marsh to sediment bank shorelines around the Albemarle-Pamlico estuarine system (APES) for a series of historical (decadal to 50-year) and short-term (bimonthly) time periods as well as for individual storm events. Long-term (historical) SCRs of approximately -0.5 ± 0.07 m year^{-1} are observed, consistent with previous work along estuarine shorelines in North Carolina. Short-term SCRs are highly variable, both spatially and temporally, and ranged from 15.8 ± 7.5 to -19.3 ± 11.5 m year^{-1} at one of the study sites. The influence of wave climate on the spatial and temporal variability of short-term erosion rates is investigated using meteorological observations and coupled hydrodynamic (Delft3D) and wave (SWAN) models. The models are applied to simulate hourly variability in the surface waves and water levels. The results indicate that in the fetch-limited APES, wind direction strongly influences the wave climate at the study sites. The wave height also has an influence on short-term SCRs as determined from the wave simulations for individual meteorological events, but no statistical correlation is found for wave height and SCRs over the long term. Despite the significantly higher rates of shoreline erosion over short time periods and from individual events like hurricanes, the cumulative impact over long time periods is low. Therefore, while the short-term response of these shorelines to episodic forcing should be taken into account in management plans, the long-term trends commonly used in ocean shoreline management can also be used to determine erosion setbacks on estuarine shorelines.

Keywords Estuarine shorelines · Shoreline erosion · Storms · Estuarine sediments · Coastal management · Hydrodynamic and wave modeling

Communicated by David K. Ralston

✉ Devon O. Eulie
  eulied@uncw.edu

1   Institute for Coastal Science and Policy, East Carolina University, Greenville, NC 27858, USA

2   Department of Geological Sciences, East Carolina University, Greenville, NC 27858, USA

3   UNC Coastal Studies Institute, Wanchese, NC 27981, USA

4   Department of Civil Engineering, Queen's University, Kingston, ON, Canada

5   Present address: Department of Environmental Studies, University of North Carolina, Wilmington, NC 28403, USA

Introduction

Estuarine shorelines are dynamic coastal features that are naturally shaped by a combination of hydrodynamic and biogeomorphic processes (Camfield and Morang 1996; Komar 1983; Roman and Nordstrom 1996; Phillips 1986; Riggs and Ames 2003). Processes such as sea level change, tectonic activity, tides, waves, and coastal storms can operate on varying temporal and spatial scales to influence the location of the shoreline and its morphology (Bellis et al. 1975; Camfield and Morang 1996; Esteves et al. 2006; List et al. 2006; Pajak and Leatherman 2002; Zhang et al. 2002). Changes in shoreline position over small spatial scales (e.g., 1 m to 10 km) and time scales ranging from hours to decades

are primarily a function of hydrodynamic processes, human activities, sediment supply, and shoreline composition (Ali 2010; Bellis et al. 1975; Camfield and Morang 1996; French 2001; Jackson and Nordstrom 1992; Phillips 1986; Riggs and Ames 2003). This variability in the spatial and temporal scales that these processes operate over can make it difficult for coastal managers to address shoreline erosion.

Shoreline change data is becoming more available to both the public and coastal managers and can help identify areas and structures at risk to erosion (Douglas et al. 1998; NRC 2007). Studies of oceanfront shoreline change are numerous, and historical or *long-term* rates of erosion are commonly used by managers to determine building setback regulations in state coastal management plans (CMPs; Crowell et al. 1993; Douglas et al. 1998). Rates of estuarine shoreline change have been less studied, and few states have setback regulations that incorporate projected shoreline loss (NRC 2007). In North Carolina, there is about 20,000 km of estuarine shoreline compared to approximately 520 km of oceanfront beaches (McVerry 2012). This includes 16,945 km of estuarine wetlands (marshes and riparian swamps; McVerry 2012). This sheer length of estuarine shoreline represents a large gap in management efforts between estuarine and oceanfront shores. In particular, wetlands are a critical habitat and there is concern regarding their potential loss. Studies also indicate that the rate of erosion along estuarine shorelines can exceed that of oceanfront shores (Corbett et al. 2008; Cowart et al. 2011; NRC 2007; Stevenson and Kearney 1996; Stirewalt and Ingram 1974). Previous studies have observed rates of change along estuarine shorelines of North Carolina from −0.5 to over −3.0 m year^{-1} (Bellis et al. 1975; Cowart et al. 2011; Riggs and Ames 2003; Stirewalt and Ingram 1974). In the Neuse River estuary, a tributary of Pamlico Sound, Cowart et al. (2011) observed a mean rate of shoreline change on the order of −0.6 m year^{-1}.

Historical shoreline change rates provide an average picture of long-term coastal change while minimizing the uncertainty associated with mapping methods (Crowell et al. 1993; Fletcher et al. 2003). Setbacks or management plans based on these rates may not account for large, episodic events such as storms or seasonal variation in the shoreline position, both of which can be significant in terms of erosion (Crowell et al. 1993; Douglas et al. 1998; Douglas and Crowell 2000; List et al. 2006). These plans often apply a mean rate of change to long stretches of coastline and commonly do not take into account fine-scale spatial variability.

Shoreline change is thought to be controlled by the complex interaction of processes and shoreline characteristics that can be highly location-specific. Differences in fetch, nearshore bathymetry, and shoreline morphology have all been shown to influence the rate of change (Cowart et al. 2011; Hardaway 1980; Phillips 1986; Rosen 1980; Schwimmer 2001; Stevenson and Kearney 1996; Wilcock et al. 1998). Wave energy has also previously been recognized to influence the rate of shoreline change (Riggs and Ames 2003; Schwimmer 2001; Cowart et al. 2011). For example, in the nearby Neuse River estuary, Cowart et al. (2011) determined an empirical relationship between wave energy exposure and the rate of erosion.

Coastal storms are also commonly indicated as drivers behind episodic, but significant erosion of shorelines (Camfield and Morang 1996; Dolan et al. 1978; List et al. 2006; Phillips 1999). Studies on oceanfront coasts highlight the ability of storms to remove large volumes of sediment from beaches and also indicate the potential for subsequent recovery of those sediments during the quiescent period following a storm event (Dolan et al. 1988; Dolan et al. 1978; Douglas and Crowell 2000; List et al. 2006; Phillips 1999). List et al. (2006) noted the existence of storm-driven "erosion hotspots." These hotspots represent segments of shoreline that are characterized by a significantly higher rate of short-term erosion then surrounding segments of the same type and morphology (List et al. 2006).

The objective of this study is to examine shoreline change over a range of temporal and spatial scales to investigate the following:(1) controls on spatial and temporal variability in shoreline position and (2) the contribution of episodic storm events to rates of shoreline change. This was accomplished by field surveys using real-time kinematic (RTK) GPS, heads-up digitizing of historical shorelines, and a coupled hydrodynamic-wave model.

Site Description

Five sites around the Albemarle-Pamlico estuarine system (APES) were chosen based on shoreline characteristics, accessibility, and location (Fig. 1). All sites were located in estuarine locations and within the boundaries of parklands, wildlife refuges, and preserves with no nearby coastal structures that might influence shoreline changes. The sites encompass a range of shoreline types, shore morphologies, land cover, and exposure to waves. Two sites were located on back-barrier shorelines, while the other three sites were located along the mainland estuarine coast.
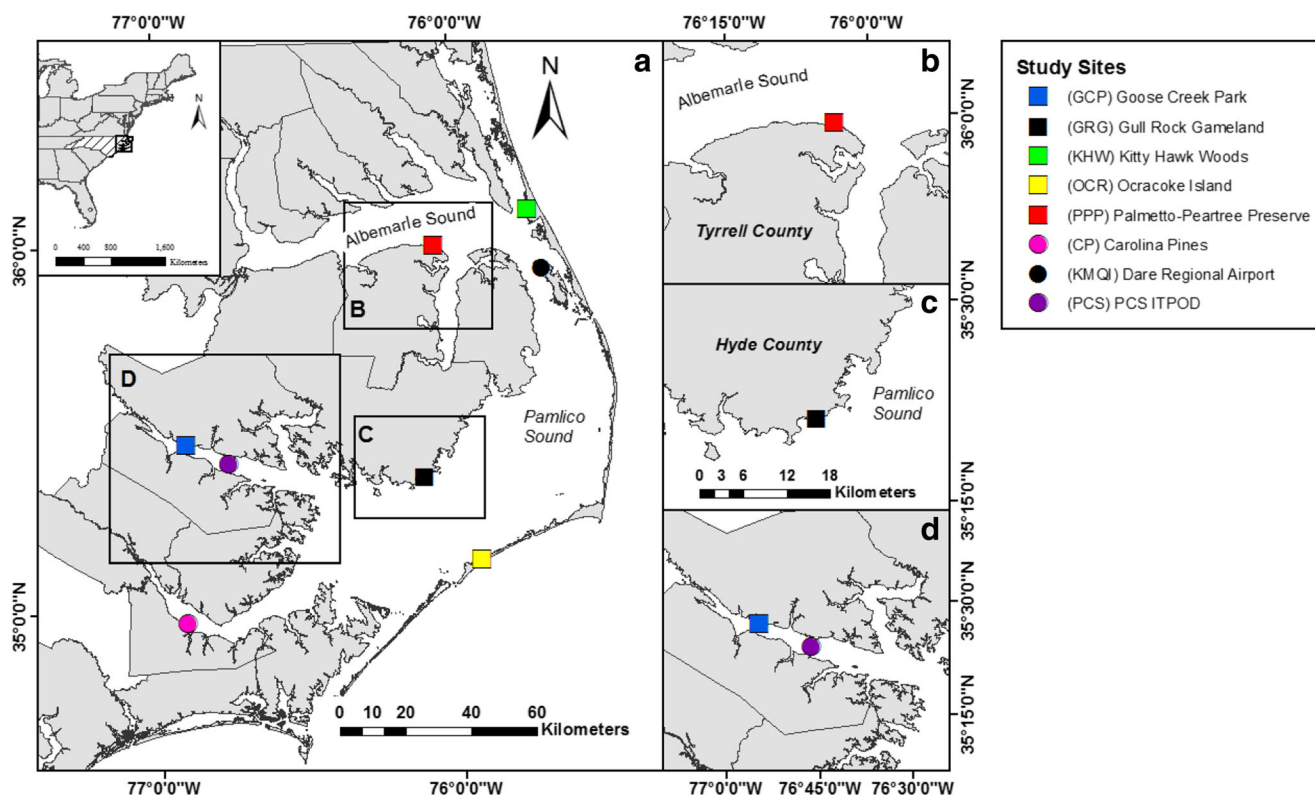
Fig. 1 *A–D* Map of locations utilized in this study. The full name for each site and abbreviated site initials are provided. The five shoreline sites are denoted by the *squares* (GCP, GRG, KHW, OCR, and PPP). The two

sites used in the wave model validation are CP and PCS, and the source of wind data for the 2010–2011 period is station KMQI (all represented by *circles*)

The first mainland site, in Goose Creek State Park (GCP), is located on the north shore of the Tar-Pamlico estuary in Beaufort County (Fig. 1). This site consists of a sandy, low-sediment bank shoreline with fringing grasses; isolated pockets of marsh; and some trees. The adjacent nearshore is shallow (<1 m), and large mobile sand shoals were present at times during the study. This site also had the most limited fetch due to estuary geometry (Fig. 1). The second mainland site, Gull Rock Game Lands (GRG), is located on Pamlico Sound in Hyde County (Fig. 1). This has a marsh shoreline characterized by a sharp subaqueous vertical scarp (generally <1 m) and an erosional morphology with extensive cleft-and-neck formations, undercutting, and pocket beaches analogous to that described by Schwimmer (2001). The site is also backed by a man-made canal system. The third mainland site is the Palmetto-Peartree Preserve (PPP), which lies on Albemarle Sound in Tyrrell County (Fig. 1). This site consists of a sediment bank and swamp forest shoreline characterized by scattered woody debris, tree stumps, and some fringing grasses. Marshes are present in isolated pockets sheltered by large cypress trees and remnants of larger peat deposits. The adjacent nearshore is

shallow (<1.5 m) and covered largely with sandy sediments and littered with woody debris.

The first of the two back-barrier sites is in the Kitty Hawk Woods Estuarine Research Reserve (KHW), located along the northern Outer Banks (Fig. 1). The shoreline consists of alternating marsh platforms and pocket beaches that lie along a wooded coast. The second back-barrier site is on Ocracoke Island (OCR), just north of Ocracoke Village (Fig. 1). The site consists of two distinct sections: one dominated by sandy sediments and a gentle slope with less dense vegetation and the other section is salt marsh with a subaqueous scarp of 20–30 cm and bisected by wide (5 to 10 m across), shallow, tidal creeks with a sandy bottom. These two back-barrier sites are not discussed in detail due to data gaps in short-term shoreline positions.

This research focuses mainly on a detailed analysis of shoreline change at the three mainland sites (GCP, GRG, and PPP). These sites were chosen for their contrasting morphology, fetch limitation, and shoreline type. The GRG and PPP sites have opposite shoreline orientations (southeast-facing and north-facing, respectively) and represent the two most common shoreline types in the APES, marsh, and sediment bank. These sites are

Table 1 Shoreline measurement dates and properties

Eras	Shoreline dates	Mean total era uncertainty (m/year)
Historical eras (H)		
50 years	1950s–2006/2007	0.1
H1	1950s–1982	0.2
H2	1982–1993	0.8
H3	1993–1998	2.2
H4	1998–2006/2007	0.9
Short eras (S)		
S	June 2010–May 2011	0.6
S1	June 2010–August 2010	3.6
S2	August 2010–October 2010	3.1
S3	October 2010–January 2011	2.5
S4	January 2011–March 2011	2.9
S5	March 2011–May 2011	3.1

Historical shoreline eras are designated by letter "H" and the short-term surveys with letter "S" to indicate short time periods

also exposed to some of the longest fetch across the large sounds. The GCP site, in contrast, is the most fetch-limited of all the study sites and has a combination of marsh and sediment bank shoreline types.

Methods

Shoreline Mapping

Shoreline position was mapped at the five study sites over multiple time periods. Table 1 lists the dates and properties of shoreline position data for each time period, hereafter referred to as "eras." Long-time period (historical 50-year and decadal) eras are designated by letter "H" and short-term (recent bimonthly) eras by letter "S" (Table 1). The historical shoreline positions were digitized from aerial photos, and the short-term eras were obtained from a series of in situ surveys that were conducted every 2 months from June 2010 to May 2011. Due to technical and logistical difficulties, the timing and duration of the short-term S1 and S2 eras at the OCR site do not match the rest of the study site eras.

At each site, approximately 5 km of shoreline from historical aerial photos was digitized using the method of Geis and Bendell (2010). Aerial photos from the 1950s and 1982 were obtained from the US Department of Agriculture (USDA) repository and the US Geological Survey (USGS) online portal. Digital orthophoto quarter quadrangle (DOQQ) images for 1993 and 1998 were obtained from the North Carolina Department of Transportation (NCDOT) GIS portal. The most recent shoreline (digitized using aerial images) used 2006 or 2007 county photos and was completed as part of a larger

shoreline mapping project for the North Carolina Division of Coastal Management (NCDCM). The 1950s and 1982 tagged-image-formatted (tif) images were imported into ArcGIS 9.3.1 and georeferenced with ground control points (a minimum of 9) from the 1998 DOQQ and 2006/2007 county images using a second-order polynomial transformation following the methodology of Cowart et al. (2011). The average root-mean-square error (RMSE) for all of the georeferenced images (averaged across all image tiles) was 1.7 m.

In situ measurements of shoreline position at the study sites were collected every 2 months from June 2010 to May 2011. During each site visit, the shoreline position was surveyed using a Trimble 5800 RTK-GPS system along a 1-km stretch of shoreline. The location of the shoreline was determined by the same criteria used in digitizing the historical shoreline positions, using the wet/dry line, the edge of the marsh platform, or the line of stable vegetation depending on the character of the shore (Geis and Bendell 2010). The RTK-GPS base station position was post-processed using the National Oceanic and Atmospheric Administration's (NOAA) automated processing system, Online Positioning User Service (OPUS). The data was processed with the "static" (>2-h record) option, and then shoreline points were re-projected using the OPUS-generated base station coordinates. Mean positional uncertainty for the RTK-GPS in this study was calculated to be ±0.4 m (Table 2). The final shoreline position points were used for the calculation of shoreline change rates.

Shoreline Change Rate and Uncertainty

Calculations of shoreline change obtained from the different methods were completed using the Analyzing Moving Boundaries Using R (AMBUR) package (Jackson et al. 2012). The end-point method was used to measure change in the shoreline position over the eras of this study. A double-baseline method is used by AMBUR to create transects for calculating change across the shoreline envelope (Jackson et al. 2012). These were created in ArcGIS 9.3.1 by buffering the innermost and outermost shorelines (buffer distances based on geometry and width of the shoreline

Table 2 Calculated (using Eq. 1) values for total uncertainty (U_t) for each type of aerial image or method utilized in this study

Method	Horizontal uncertainty (m)
1950s images	±3.0
1982 images	±2.9
1 m 1993 and 1998 DOQQs	±7.7
0.3 m 2006/2007 orthophotos	±2.4
Aerostat images	±0.4
RTK-GPS	±0.4

envelope for each set of historical and short-term eras). Shoreline transects were placed at 1-m intervals along the double baseline at each site. While testing at two of the sites indicated coarser transect spacing of 5, 10, 25, and 50 m would result in mean site shoreline change rates (SCRs) that were not significantly different, the fine scale of 1-m transect spacing was deemed more appropriate for examining intra-site variability.

The uncertainty (U_t) associated with the annualized SCR for each era was calculated for each of the methods (i.e., orthophotos and the RTK-GPS surveys) using the following equations (Cowart et al. 2010; Crowell et al. 1993; Eulie et al. 2013; Fletcher et al. 2003; Gentz et al. 2007):

$$U = \sqrt{E_d^2 + E_r^2 + E_g^2 + E_u^2} \qquad (1)$$

where E_d is the digitizing error, E_r is the image rectification error, E_g is the RTK-GPS instrument measurement error, and E_u is the uncertainty associated with surveying the shoreline (as determined by calculating the mean difference in shoreline position from repeated surveys at each site). The error for each individual shoreline survey (U_{ti}), where i represents a particular era, was used to determine the annualized uncertainty (U_t) for each era by

$$U_t = \frac{\sqrt{U_{t1}^2 + U_{t2}^2}}{T} \qquad (2)$$

where T is the total length of time included in the era (Anders and Byrnes 1991; Crowell et al. 1993; Fletcher et al. 2003). The mean U_t for each era is reported in Table 2. Individual U_t values are provided for each shoreline change rate. Calculating the total uncertainty associated with reported shoreline change rates provides a measure of confidence for the data (Crowell et al. 1993; Moore 2000). The mean U_t is foremost dependent on the error associated with each set of imagery (or in situ surveys) and the length of time over which it is annualized (Crowell et al. 1993). Shoreline derived from older aerial imagery are less accurate due to characteristics such as lower resolution, the accuracy of ground control points (georeferencing), and the accuracy of older GPS equipment. However, as is seen in shoreline change time series data, the longer the time frames of the data, the lower the annualized error or uncertainty (Crowell et al. 1993; Fletcher et al. 2003). For comparison, a U_t value determined by Cowart et al. (2010) for a 40-year era of shoreline change at Cedar Island, North Carolina, was found to be very close to the 50-year-era U_t for this study (0.05 and 0.07 m year^{-1}, respectively). The difference between these specific U_t values was due to the image rectification error (E_r), for the oldest photographs, whereas the recent short time periods may be more accurate in terms of shoreline position due to modern imagery and GPS equipment, but as T is much smaller, U_t can still be high.

Meteorological Observations

Hourly wind speed and direction observations for the 2010–2011 short-term eras were obtained from station KMQI (Manteo, NC; Fig. 1). Wind records from Cherry Point Marine Corps Air Station (MCAS) and station KHSE (Cape Hatteras; Fig. 1) were used to model waves for time periods with simultaneous in situ observations (14–16 September 2005 and 26–28 August 2011). All wind speed observations are reported in meters per second and wind direction in the nautical convention (from direction) as degrees from the geographic north. The wind record from station KMQI was filtered to remove hours where no data was available. Table 3 summarizes the percentage of time, and there is no hourly wind data per short-term era for the GRG and PPP sites, with the greatest amount of missing data in late December 2010 to early January 2011. This time period occurred during the S3 and S4 short-term eras (Table 3).

Wave Modeling

This study uses a numerical model to simulate waves in the APES for specific wind events that occurred during the short-term time periods. The model consists of a series of modules that can be utilized individually or coupled to simulate currents, water levels, waves, and other parameters in shallow coastal or inland waters (Lesser et al. 2004). The Delft3D FLOW model is used to simulate hydrodynamics and is coupled to the SWAN (Simulating WAves Nearshore) surface WAVE model (Booij et al. 1999). SWAN is a third-generation, spectral wave model based on the action balance equation. The model was applied to the APES system by Mulligan et al. (2015) to simulate the waves and storm surge of Hurricane Irene that directly impacted the region on August 2011. The model uses a rectilinear computational grid with a horizontal grid resolution of 250 m, with water depths

Table 3 The percent of time (hourly) per era that there is no wind data available for the GRG and PPP sites

Eras	Percent time of no wind data	
	GRG	PPP
S1	6.0	5.6
S2	10.7	11.4
S3	11.5	17.0
S4	22.4	19.0
S5	5.3	5.5

The percentages were calculated using the number of hours of available wind data and the total number of hours in each era. The majority of hours where wind data was unavailable occurred between December 2010 and January 2011

interpolated from bathymetric data provided by NOAA. The grid was then projected in spherical coordinates (latitude and longitude). The model is set up using hydrodynamic constants (e.g., bottom roughness, eddy viscosity) and wave parameters (e.g., bottom friction, whitecapping, wave breaking) determined by Mulligan et al. (2015) for the APES. The model results in the present study are validated by comparison with wave observations at Carolina Pines (CP) in the Neuse River estuary during Hurricane Ophelia in 2005 and at site PCS in the Tar-Pamlico estuary (locations shown in Fig. 1) during Hurricane Irene in 2011. The wave observations were collected at the CP site using a Nortek Aquadopp that sampled at a frequency of 2 Hz on September 2005 and at the PCS site using a Nortek Vector that sampled at a frequency of 8 Hz on August 2011. All simulations were run using a 1-min time step with wave computations and FLOW-WAVE module coupling every 60 min. Spatially uniform winds from observations at the Cherry Point MCAS station were used to force the model. The model validation at CP and PCS is shown in Fig. 2, indicating good agreement with spectral estimates of the significant wave height (H_s) and peak period (T_p) during the storm events. The model results at the Carolina Pines (CP) site were found to be in good agreement with the observations of the Hurricane Ophelia storm event that occurred on 14–15 September 2005 (Fig. 2a, b). The model slightly underestimated significant wave height (H_s) and peak wave period (T_p; Fig. 2a, b). The maximum predicted H_s was 1.1 m (observed H_s = 1.3 m) and the predicted T_p was 3.3 s (observed T_p = 3.7 s). Model validation for Hurricane Irene also

indicates a good agreement between the predicted and observed values (Fig. 2c, d), with predicted maximum H_s = 1.7 m (observed H_s = 1.8 m) and predicted T_p = 3.6 s (observed T_p = 3.6 s; Fig. 2c, d).

A series of simulations were run for three meteorological events during a period of high shoreline erosion rates (S2 era) in order to gain an understanding of the wave energy at the mainland study sites (GCP, GRG, PPP). The first event was the passage of Hurricane Earl offshore of the NC coast in the early September (2–3 September 2010) with wind speeds of up to 17 m s^{-1} measured at the KMQI station (location shown in Fig. 1). Event 1 and Event 2 were frontal storms with wind speeds of >6.0 m s^{-1} that occurred during 16–17 September 2010 and 27 September–4 October 2010. Wind speeds of <6.0 m s^{-1} have been shown in other fetch-limited systems to result in relatively low wave conditions (<0.2 m) and were not included in these simulations (Jackson et al. 2012; Pierce 2004).

An idealized simulation was run to examine the distribution of wave energy over different wind directions and speeds at the study sites, hereinafter referred to as the "wind ramp," and used to hindcast the long-term wave climate at the GRG and PPP sites. The wind ramp was not examined at the GCP site due to its similar orientation to the GRG site shoreline (both are most exposed to southerly wind directions), and the GCP site is located at the upper reach of the Tar-Pamlico tributary where fetch is more limiting (Fig. 1). Wind inputs were developed using wind speeds ranging from 6 to 30 m s^{-1} in 2 m s^{-1} increments for each of the eight cardinal and ordinal

Fig. 2 Comparison of wave observations and model results at the CP site for Hurricane Ophelia, on 14–16 September 2005 (**a** significant wave height; **b** peak wave period), and at the PCS site for Hurricane Irene, on 26–28 August 2011 (**c** significant wave height; **d** peak wave period)
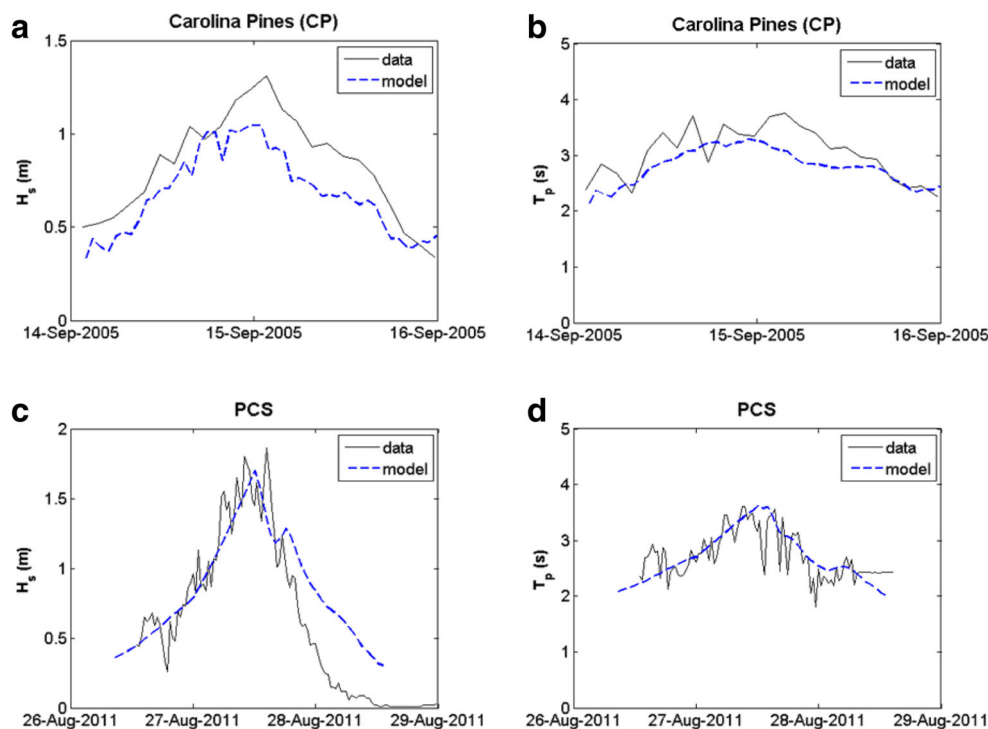
compass directions (e.g., north, north-northeast, northeast). The results for this simulation were then matched to the actual 335-day-long wind record for all of the short-term eras (June 2010–May 2011). The hourly wind record from station KMQI was filtered, and then each hour was matched with the analogous simulation result for that wind speed bin and compass direction.

Statistical Analysis

Descriptive statistics and tests were calculated using the Minitab software package. Analysis of variance (ANOVA) tests were conducted at a significance level of $P \leq 0.05$ to identify if rates of change were significantly different between the five study sites and between different eras within each site. Pairwise comparisons were made using Tukey's honestly significant difference (HSD) test.

Results

Temporal and Spatial Variability in Shoreline Change

Over the 50-year historical era, all of the study sites exhibited erosion and at a rate that exceeded the calculated mean uncertainty of ± 0.1 m year^{-1} (Table 1, Fig. 3(A–E)). Four of the sites, GCP, GRG, OCR, and PPP, had rates of change of approximately -0.5 m year^{-1} (-0.5 ± 0.3, -0.5 ± 0.5, -0.6 ± 1.2,
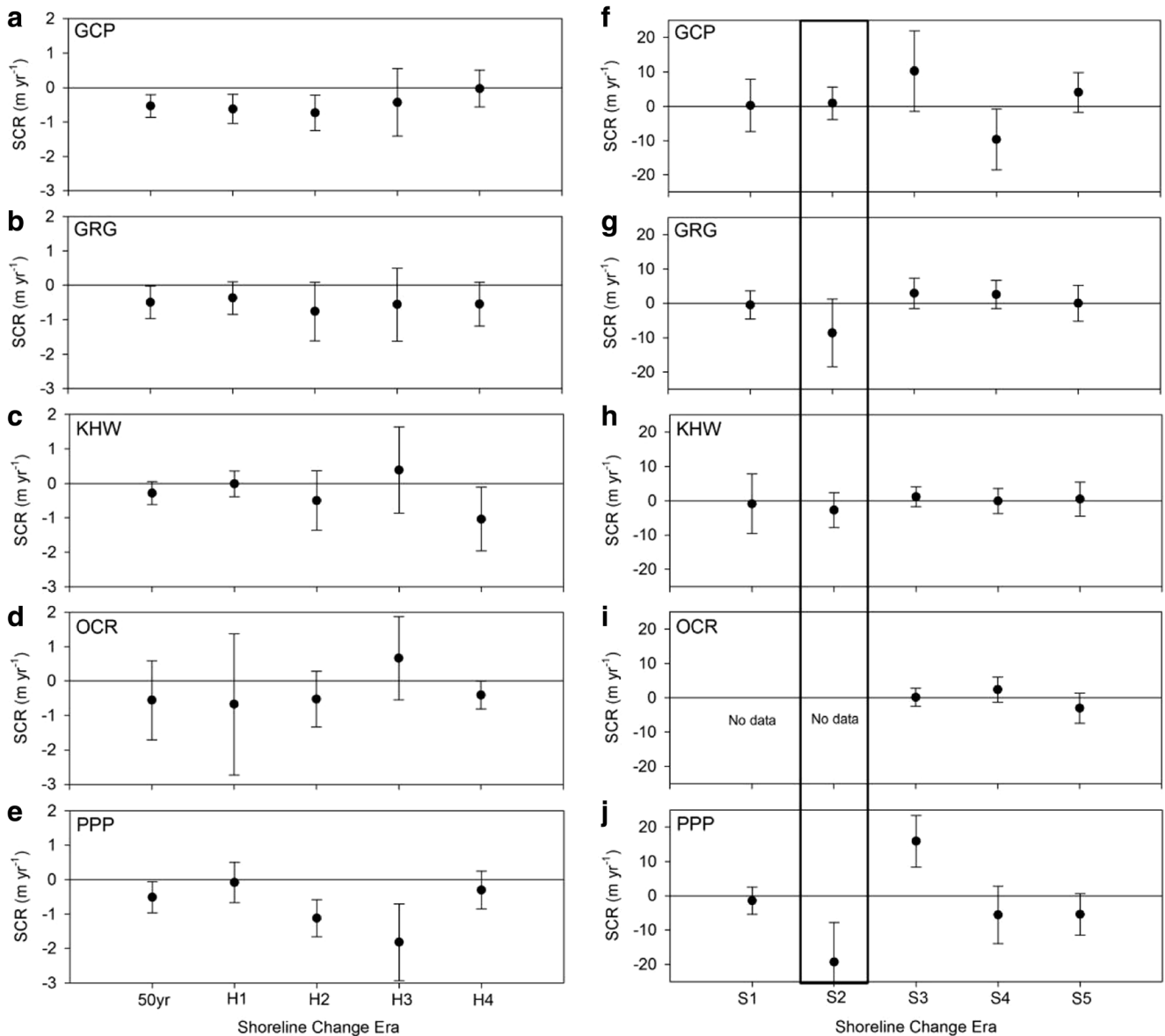
Fig. 3 *A–E* Mean shoreline change rates (*SCRs*) for all of the study sites and for all historical time periods (*eras*; see Table 1). *F–J* Mean SCRs for all of the study sites and for all of the short time periods. *Error bars* represent 1 standard deviation. Negative SCRs are indicative of erosion and positive SCRs indicate accretion. The *box* indicates an era in which Hurricane Earl occurred

and -0.5 ± 0.5 m year^{-1}, respectively). In contrast, the KHW site showed significantly less erosion, with an SCR of only -0.3 ± 0.3 m year^{-1} for the 50-year era. In pairwise comparisons, the OCR site had a significantly greater rate of erosion than all but the GCP site, but it also had the greatest variability with a standard deviation of ± 1.2 (Fig. 3(A–E)).

Rates of shoreline change were also examined over the following individual eras: within the 50-year period, a multi-decadal era of approximately 30 years (H1), two individual decades (H2 and H4), and a 5-year era (H3). The dates for each of these eras and their calculated uncertainty (U_t) are reported in Table 1. Overall, SCRs for the H1–H4 eras were highly variable, by era and site. Rates of change were most consistent at the GRG site over all of the historical eras and only ranged from -0.4 ± 0.5 to -0.8 ± 0.8 m year^{-1} (Fig. 3(B)). In contrast, the PPP site exhibited some of the greatest variability (-0.1 ± 0.6 to -1.8 ± 1.1 m year^{-1}) and the OCR site had the greatest era (H3) of accretion (0.7 ± 1.2 m year^{-1}; Fig. 3(D, E)).

During the H1 era (1950s to 1982), all of the sites exhibited erosion. The GCP, GRG, and OCR sites had rates of change that exceeded the uncertainty of ± 0.2 m year^{-1} (Fig. 3(A, B,

D)). In contrast, the KHW and PPP sites had minimal erosion that was well within the error, indicating little average change at either location. For the H2 era, all of the sites exhibited rates of change that exceeded the long-term (50-year) average SCR but were within the U_t for this era (H2), with the exception of the PPP site; the PPP site had an SCR of -1.1 ± 0.5 m year^{-1} (Fig. 3(E)). During the H3 era (1993–1998), rates of shoreline change were variable and included the only positive SCRs during the 50-year period; the two back-barrier sites, KHW and OCR, both exhibited mean accretion. The SCR at site PPP was significantly higher than the 50-year average and represented the greatest erosion rate observed during all of the historical eras of -1.8 ± 1.1 m year^{-1} (Fig. 3(E)). During the most recent historical era of approximately a decade (1998–2006/2007, H4), all sites exhibited erosion and, similar to the H3 era, the SCR at only one site, KHW (-1.0 ± 0.9 m year^{-1}), had measurable change beyond the annualized error.

The short time periods (S1–S5) exhibited a tendency to alternate between erosion and accretion depending on the site (Fig. 3(F–J)). It should be noted that there is no data for the OCR site until the S3 era. During the S2 era, there was

Fig. 4 Shoreline change at the PPP site. **a** Shoreline change over the 50-year era. **b** Shoreline change over the modern (S1–S5) era. The spatial extent of **b** is indicated by the *black rectangle* in **a**. The plots located *below each map* indicate erosion (*red blocks*) or accretion (*blue blocks*) averaged over 50 m along the shoreline. The plots show the era along the *y-axis* and the alongshore transect number along the *x-axis*
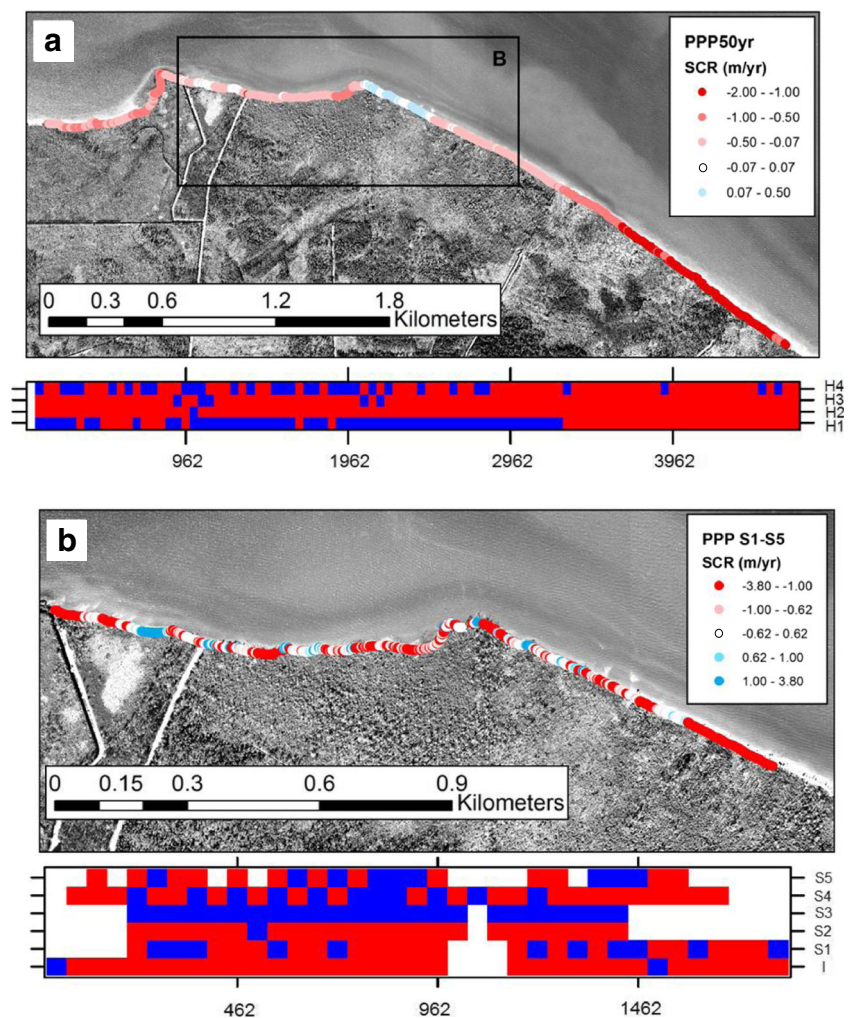
significant change at the GRG and PPP sites of -8.6 ± 9.8 and -19.3 ± 11.5 m year^{-1}, respectively, that exceed the annualized error of ± 3.1 m year^{-1} (Fig. 3(G, J)). After this period of high erosion, the S3 era was characterized by accretion at all of the sites. However, the accretion was only statistically significant at the two sediment bank sites, GCP and PPP (10.3 ± 11.7 to 15.8 ± 7.5 m year^{-1}; Fig. 3(F, J)). At the GCP site, this was due to significant accretion along a segment of the shoreline. This accretion widened a small section of the shoreline by over 10 m. At the PPP site, the greatest accretion was also localized to a small segment of the shoreline. For both the GCP and PPP sites, this period of accretion was followed by another era (S4) of erosion, with SCRs of -9.7 ± 8.8 and -5.6 ± 8.4 m year^{-1}, respectively (Fig. 3(F, J)). Finally, historical and annualized short-term SCRs were compared for all study sites. In pairwise comparisons, historical versus annualized SCRs were found to be significantly different from each other at all five study sites ($P < 0.01$).

There was distinct alongshore variability in the rates of change due to shoreline geometry, orientation, composition, and vegetation at each study site. Over the historical eras, alongshore patterns in shoreline change were relatively consistent at individual sites. For example, the highest (50-year) rates of shoreline erosion at the PPP site (>1.0 m year^{-1}) were consistently observed across transects ~3500–5000 (Fig. 4a). Distinct patterns of shoreline change were also noted between transects 1 and 2500, where the shoreline forms a series of headlands. The GCP and GRG sites also exhibited distinct patterns of shoreline change. At the GRG site, the highest erosion occurred along a section of shoreline between transects 3800 and 4000 (Fig. 5a). This segment of shoreline was backed by a shore-parallel canal first in 1972 imagery, but not present in the 1956 imagery. Over the subsequent decades, erosion removed the fronting section of marsh platform, exposing the canal and its shoreline to Pamlico Sound. Over the short eras, spatial trends were less clearly defined at some of the sites due in part to the higher uncertainty values and

Fig. 5 Shoreline change at the GRG site. **a** Shoreline change over the 50-year era. **b** Shoreline change over the modern (S1–S5) era. The spatial extent of **b** is indicated by the *black rectangle* in **a**. The *bars below* **a**, **b** indicate the alongshore transect number
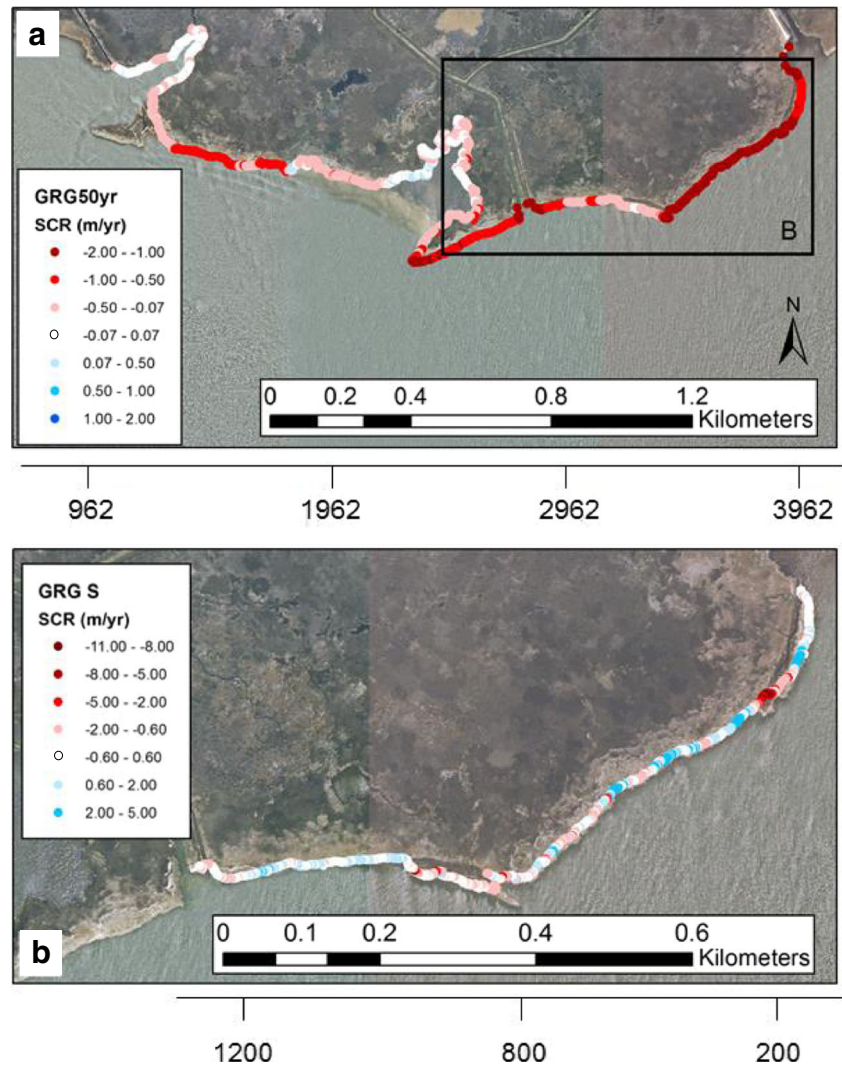
greater temporal variability. Segments of shoreline that were clearly defined as consistently eroding over the 50-year era were observed to erode, accrete, or have no change depending on the short-term era. For example, at the GRG site between transects ~3800 and 5000, the historical eras exhibit consistently high rates of shoreline erosion (Fig. 5a, b). In contrast, during the short eras, the same shoreline is characterized by alternating segments of erosion, no observable change, or even minor accretion (Fig. 5a, b).

Wind and Waves

Waves are recognized as one of the main drivers of shoreline erosion in the APES (Bellis et al. 1975). The coupled hydrodynamic-wave model was run for three meteorological events that occurred during the S2 period of high erosion and an idealized wind ramp simulation. The results from the initial three simulations of meteorological events are illustrated in Figs. 6 and 7. The overall greatest significant wave heights occurred at the PPP site from the passage of Hurricane Earl in the early September (Fig. 6(B)). As the storm passed offshore, the dominant wind direction was from the north at speeds of

16–17 m s^{-1} (Fig. 6(A)). These conditions resulted in an H_s value of 1.2 m at the PPP site (Fig. 6(B)). At the GCP and GRG sites, significant wave heights were less than 0.6 m (Fig. 6(B)). This smaller value was due to the fetch limitation imposed by the wind direction (from the north) resulting in the largest wave heights along the southern shorelines of Albemarle Sound and Pamlico Sound (Fig. 7(A)). The GCP and GRG sites, on the northern shorelines of the Tar-Pamlico estuary and Pamlico Sound, were exposed to smaller waves (less than 1.0 m; Fig. 7(A)).

The second event modeled during the S2 era was for a typical frontal system that moved over the study area on 16–18 September 2010 and resulted in wind speeds of 7–9 m s^{-1} from the south during the peak of the storm (Fig. 6(E–H)). While wind speed was much lower during Hurricane Earl, the model calculated significant wave heights of over 0.5 m and wave peak periods of almost 3 s for the GRG site (Fig. 6(F, G)). The model results for the PPP and GCP sites indicated H_s of only 0.4 m and T_p close to 2 s for this same storm (Fig. 6(F, G)). Change in water level was less than 0.1 m for the duration of the event (Fig. 6(H)). The spatial distribution of significant wave heights for the peak wind speed during this event is illustrated in Fig. 7(B) and indicates that the highest H_s values

Fig. 6 Model results for the Hurricane Earl and event 1 wind events during the S2 era, at the GCP (*blue*), GRG (*dashed black*), and PPP (*dashed red*) sites. *A, E* Wind stick vectors indicating speed and direction. *B, F* Significant wave height (H_s). *C, G* Peak period (T_p). *D, H* Water level (η)
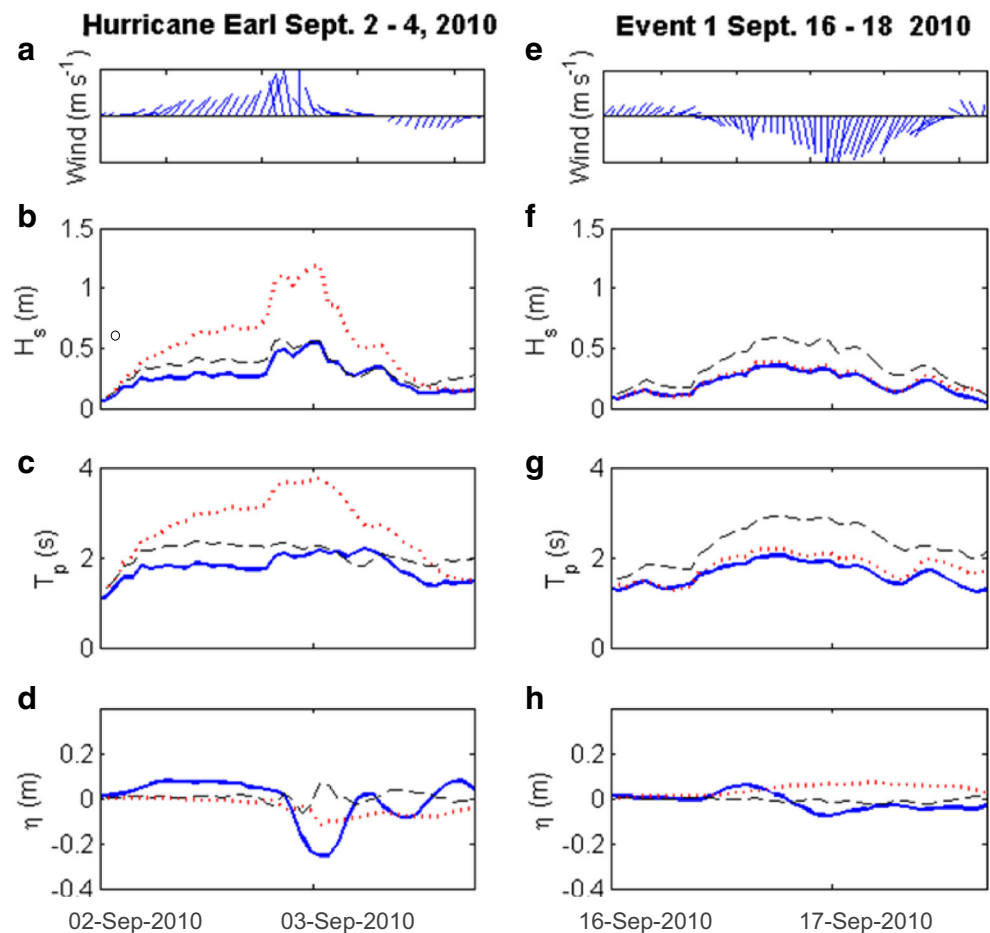
Fig. 7 Model results across the APES for significant wave height (H_s) at the GCP, GRG, and PPP sites for peak wind speed during the S2 era. A Hurricane Earl. B Event 1. C Event 2a. D Event 2b. The *arrows* indicate wind direction at each time in degrees from the true north; wind speed is indicated in meters per second
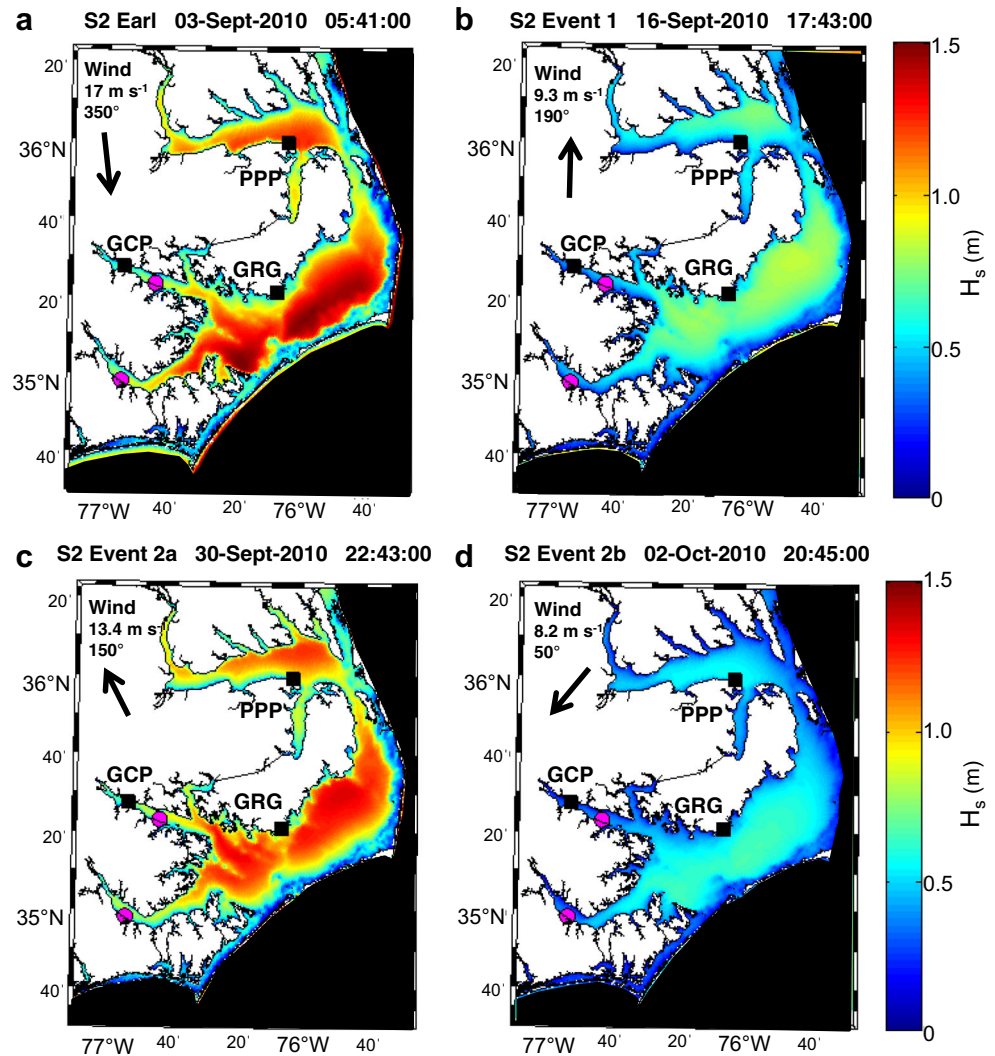

occurred along the northern shore of Albemarle Sound and along the northern and western Pamlico Sound, near site GRG.

The final event modeled for the S2 era was a week-long (27 September–4 October 2010) frontal system with winds >6 m s^{-1} and heavy precipitation that contributed to extensive coastal flooding at the three study sites. The greatest recorded wind speeds of 13.4 m s^{-1} (from the south-southeast; 150°) occurred early on 1 September 2010. This was preceded by 12 h of consistent southeast winds over 8 m s^{-1}. Due to this 12-h setup, water level was predicted by the model to have increased by 0.26 and 0.15 m at the GCP and PPP sites, respectively. As with event 1, significant wave heights were greatest during this period along the northern Albemarle Sound and Pamlico Sound (Fig. 7(C)). After 1 October 2010, the wind direction shifted to the north and the wind speed dropped to 5–8 m s^{-1} but was sustained for the next 2 days. While this resulted in overall lower wave heights across the APES, H_s at the PPP site was much higher than those calculated at the GCP and GRG sites (almost double the

significant wave heights at GCP). Greater wave heights were again along the southern shorelines of the APES, as was observed for the Hurricane Earl event (Fig. 7(D)). It is clear that wind direction over this 6-day period played a significant role in determining wave height at the different sites.

The results from the wind ramp simulation for the GRG and PPP sites are shown in Figs. 8, 9, 10, and 11. Figure 8 illustrates the role of wind direction on wave height at the two sites. The GRG site has a maximum H_s value of 1.1 m for wind from the southeast at 30 m s^{-1} (Fig. 8a), and the largest wave heights occur for wind direction from the east to the southwest, where fetch is longest (31–54 km; Fig. 8a). The PPP site exhibited a higher significant wave height of 1.7 m when the wind was from the north (fetch 18 km) at 30 m s^{-1} (Fig. 8b). Overall, the largest wave heights were simulated at the PPP site when the wind direction was from the west, south, or east with fetch of 18–33 km (Fig. 8b).

Next, the wind ramp results were matched to the wind record for all the short-term eras. At the GRG and PPP sites, 84–90 % of the time during the short-term eras (S1–S5) was
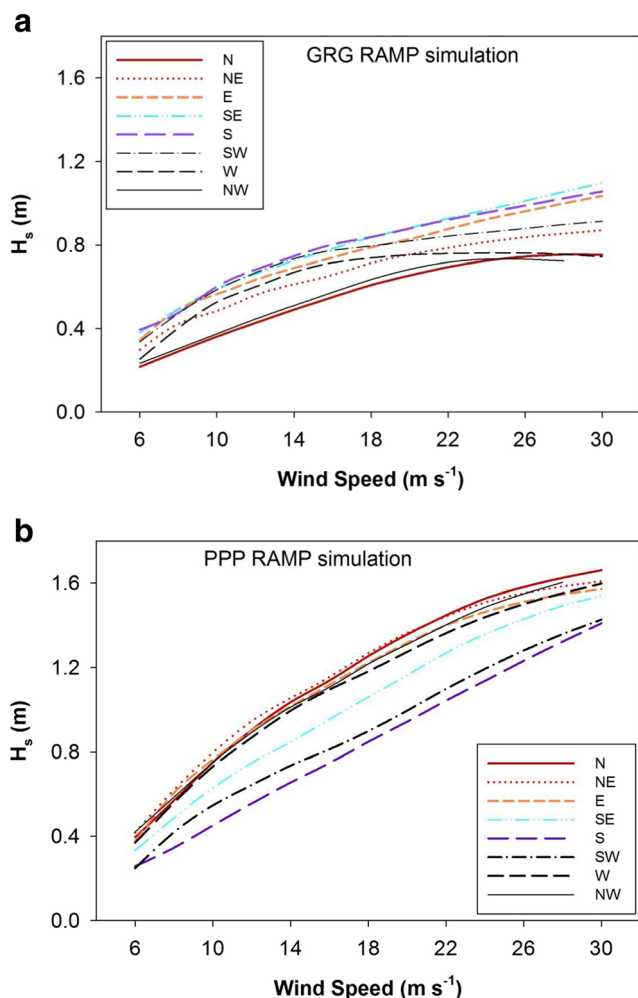
Fig. 8 Significant wave height (H_s) for each wind speed and direction in the wind ramp simulation (wind speeds 6–30 m s^{-1}, 8 cardinal and ordinal compass directions) at **a** the GRG site and **b** the PPP site

simulated to have significant wave heights of <0.4 m (Figs. 9 and 10). This demonstrates that most of time during the study, the shorelines were exposed to a climate of shorter-period (<2 s) smaller waves. The two sites experienced H_s >0.4 m at only 10–16 % of the time during the short-term eras (Figs. 9 and 10). During that time, the shoreline at each site was exposed to approximately 46–60 % of the total wave energy calculated for the entire short-term period (Fig. 10). So while a greater proportion of the total study time experienced smaller wave heights, the time periods that encompassed those less frequent, larger waves, experienced greater wave energy.

At the PPP site, the 16 % of simulated wave heights >0.4 m occurred during the S2, S4, and S5 eras when rates of erosion exceeded 5 m year^{-1} (Fig. 9). The greatest H_s (0.1 % of the time) and approximately 4 % of total wave energy (S1–S5) occurred during the S2 era when the rate of erosion was almost 20 m year^{-1} due to the influence of Hurricane Earl (Figs. 9 and 10). In contrast, during the S3 era, the shoreline returned to its pre-Earl position through the accumulation of material. Wave

heights were predominantly 0.2–0.6 m with the greatest energy from the 0.4–0.6-m bin. During the S3 and S4 eras, most wave energy was observed in the 0.6–0.8 and 0.8–1.0 H_s bins, and this was accompanied by some of the highest rates of erosion observed in the study at the PPP site (5.6 and 5.4 m year^{-1}, respectively; Figs. 9 and 10). While these results indicate a potential relationship between wave energy and erosion rate, no direct correlation was found when mean SCR was plotted against mean significant wave height (Fig. 11).

Storm Events

Shoreline position and wave climate was examined for Hurricane Earl that passed within 50 nautical miles of North Carolina on 2 September 2010. Mean SCRs of −8.6 and −19.35 m year^{-1} were measured post-Earl at the GRG and PPP sites, respectively (Table 4). The peak wind speed of the Hurricane Earl event was 17 m s^{-1} and from the north (0°), resulting in the highest significant wave heights (> 1 m) and greatest peak period (T_p; 3.8 s) along the southern shorelines of Albemarle Sound and Pamlico Sound, including the PPP site (Table 4). At the GRG site, the mean significant wave height of only 0.6 m was simulated. For comparison, during Hurricane Irene, H_s of over 1.5 m was observed at the PPP site as the storm passed over the site and winds of >30 m s^{-1} shifted from the southeast to the northwest. Mean SCRs of −9.74 and −3.84 m year^{-1} were calculated for the GRG and PPP sites, respectively. It is likely the differences in mean SCR between the two storms are the result of the differing dominant wind directions.

Discussion

Long-Term Versus Short-Term SCRs

Annualized rates of shoreline change were found to be significantly different for short-term eras in comparison to long-term eras. To examine the contribution of high erosion events, such as those captured in the short-term eras, to the long-term, cumulative change in shoreline position, the values were plotted in a linear regression model for the GCP, GRG, and PPP sites (Fig. 12; after Crowell et al. 1993). The spatial average shoreline position (SASP) for each historical era was plotted, and linear regression analysis was performed at a 95 % confidence interval. Position was plotted as the mean net change in a distance of a shoreline's position (in meters) since the initial shoreline (baseline) in 1956. Then, a linear regression model was fitted to the data points and the 95 % confidence interval band was plotted. The linear regression models were observed to fit the historical data well, as evidenced by a high r^2 value for all three sites: 0.95, 0.95, and 0.85 at the GCP, GRG, and
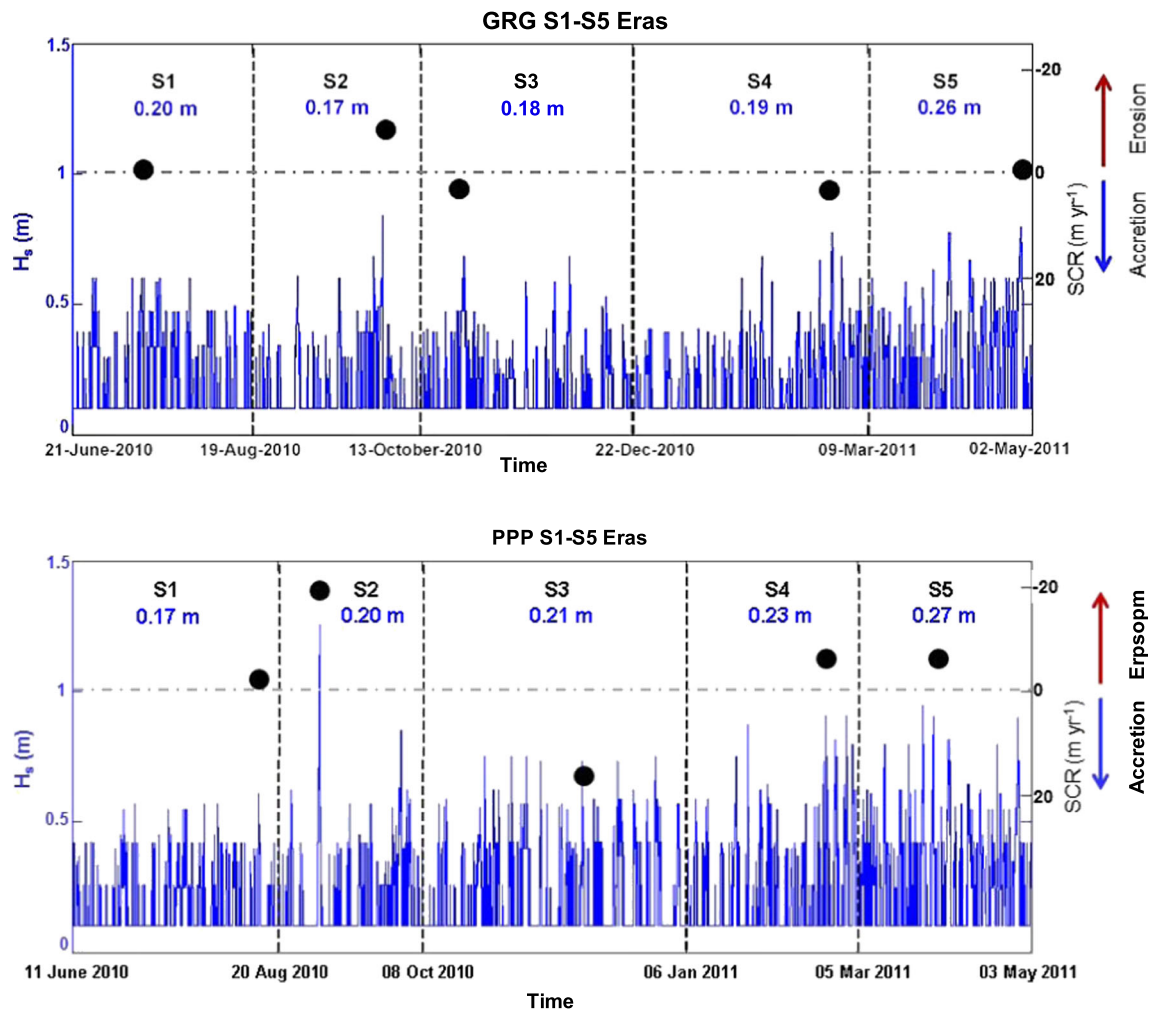
Fig. 9 Time series of wave heights using the wind ramp simulation results at the GRG and PPP sites and the annualized shoreline change rate (*SCR*, m year^{-1}) for all of the short-term eras (S1–S5). Individual eras are denoted by the *vertical dashed lines*. The *blue line* represents hourly significant wave height (H_s) as determined from the coupled hydrodynamic-wave model. Due to constraints of the model when simulating waves under low wind conditions (<6 m s^{-1}), the minimum wave height is 0.1 m. Mean H_s (*blue text*) for each era is listed in meters. The *black circles* denote the mean annualized SCR for each era. The *red arrow* indicates negative SCR values (erosion), and the *blue arrow* indicates positive SCR values (accretion)

PPP sites, respectively (Fig. 12). The SASP for each short-term era was then plotted to determine if they fell within the 95 % confidence interval band for each site (Fig. 12). All of the short-term-era SASPs were found to fall within the 95 % confidence interval band at all three sites. So, while the short-term SCR rates, and those of storm events, are significantly higher than those of the long-term eras, the spatially averaged net change in position falls within the long-term trend (Fig. 12). This indicates that these short-term cycles of erosion and accretion, as well as the high-impact but low-frequency storm events, may not have a strong impact on the long-term trend as previously thought. This is likely due to the short duration (and lower frequency) of such events. This finding represents a change in expectations on the part of the investigators as it was originally hypothesized that individual events would drive not only short-term rates but also long-term rates.

Wave Climate and Short-Term Shoreline Change

Results from the model simulations indicated a possible relationship between shoreline change rates and wave climate. However, further analysis indicates the relationship may be more complex and can be explored in the present study. At the GRG site, greater wave energy was associated with the S5 era; however, no shoreline change occurred. A study by Cowart et al. (2010, 2011) indicated the importance of shoreline characteristics such as scarp height, substrate cohesion, and vegetation type that may modify the erosion potential of marsh shorelines. At the GRG site, these factors may reduce the potential for erosion. However, during the S2 era when wave heights exceeded 0.8 m, there was significant erosion recorded at the site, suggesting that wave energy likely exceeded the threshold necessary to induce sediment erosion.
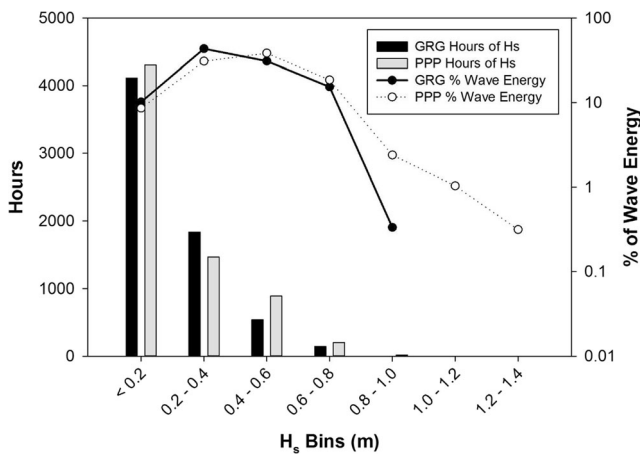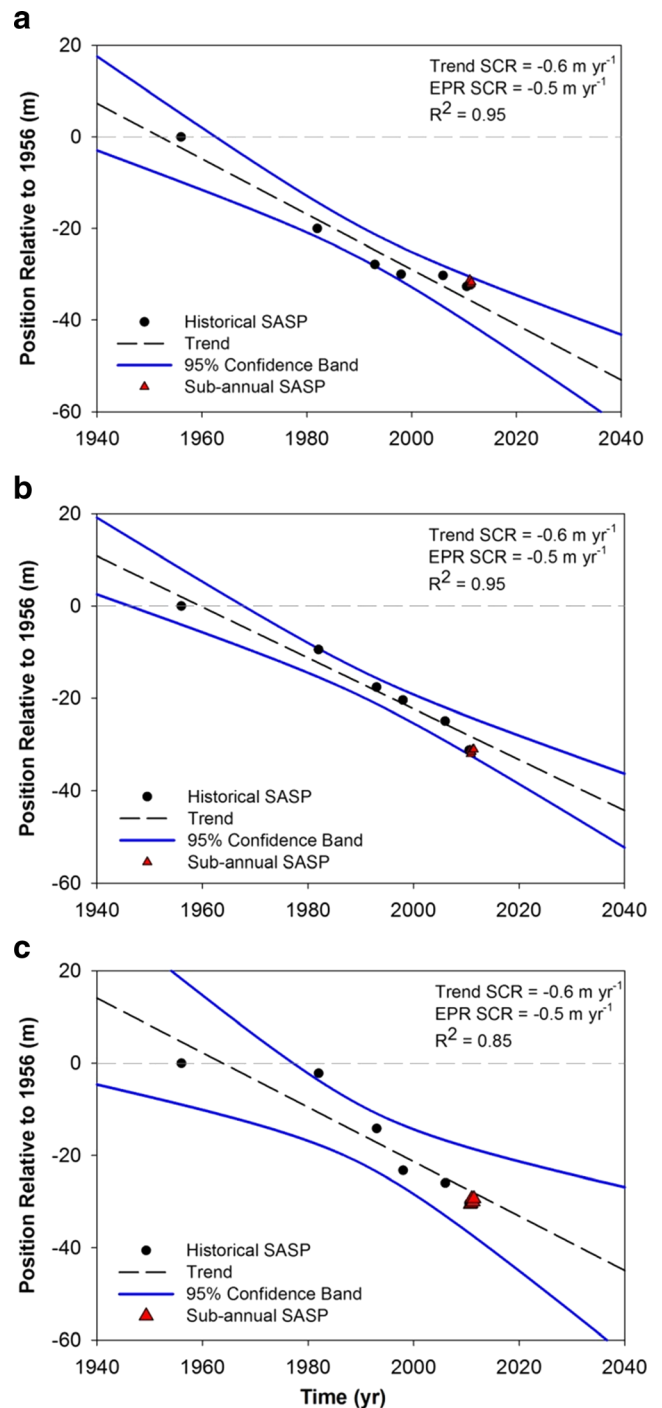
Fig. 10 Probability density distribution of hours of significant wave heights and percent of total wave energy over all of the short-term eras (S1–S5) at the GRG and PPP sites. Significant wave height divided into height bins of 0.2 m (*x-axis*) and time reported in hours (*left y-axis*). The percent of total wave energy (%; *right y-axis*) per bin is also presented. The *bars* denote hours of significant wave height for both sites, per bin. The *lines* denote percent of wave energy for both sites, per bin
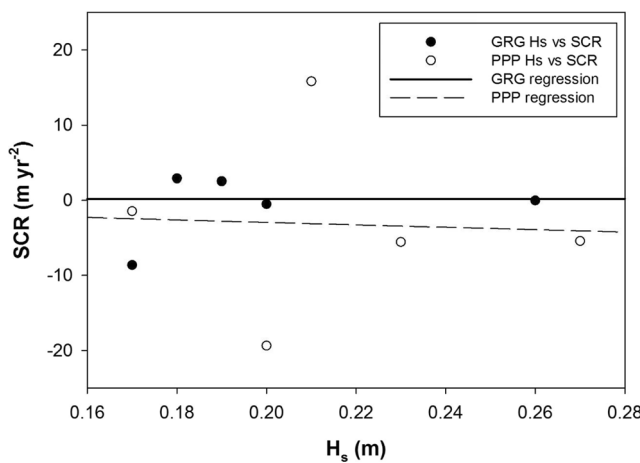
Fig. 11 Mean SCR plotted against mean significant wave height (derived from wind ramp results and wind record) for each short-term era by site (GRG and PPP)

Fig. 12 Trend in spatial average shoreline position (*SASP*) for all study eras. *A* The GCP site. *B* The GRG site. *C* The PPP site. The trend value is the SCR (m year^{-1}) calculated from the linear regression. The end-point rate (*EPR*) value is the 50-year (1956–2007) SCR (m year^{-1}) calculated using AMBUR

Table 4 Shoreline change rates and wave characteristics at the GRG and PPP sites for Hurricane Earl. Wave characteristics include significant wave height (H_s), water level (η), and peak period (T_p)

| Event	Site	SCR (m year^{-1})	H_s (m)	η (m)	T_p (s)
Hurricane Earl	GRG	−8.64	0.6	0.07	2.2
	PPP	−19.35	1.2	−0.12	3.8

The simulation results for the PPP site suggest that during periods of smaller waves, sand can move onshore, but during periods with larger waves, the critical erosion stress of marsh substrates can be surpassed, resulting in erosion. However, in the study of Cowart et al. (2010), no direct correlation between wave energy and erosion rate was observed (Fig. 11).

There is also a seasonal component to the observed trends in wave climate and shoreline change. At both GRG and PPP sites, the summer months (June–August) were characterized by consistently smaller wave heights and an absence of any significant change in shoreline position (Fig. 11). Historically, and during this study, winds are from the southwest at this time of the year, and few fronts occur (Cowart et al. 2010; Wells and Kim 1989). At the PPP site, this wind direction limits the wave development along the southern shorelines of Albemarle Sound. At the GRG site, while the fetch for wind from the southwest is large, much wave energy is likely reduced by the extensive shoals seaward of the site (Fig. 13a). During the months of September and October, the passage of tropical and extra-tropical storms can result in high-energy events (with large wave heights), but these relatively short periods can significantly erode these estuarine shorelines (Fig. 9). During the winter and early spring months (December–March), the wind is predominantly from the north and northeast, directions that were found in simulations to produce the greatest wave heights at the PPP site

and were characterized by >5 m year^{-1} of erosion (Cowart et al. 2010; Wells and Kim 1989).

As alluded to above, water depth is another factor that controls wave climate. Wave height was almost always greater at the PPP site. However, the GRG site has greater fetches of 31–54 km, in contrast to fetches of 18–33 km at the PPP site. These results from the model are likely a function of the bathymetry at the sites (Fig. 13). At the GRG site, where wave heights were simulated to be lower, the water depth is only 2.2 m, and the bathymetry shows extensive shallows with little slope (Fig. 13). Water depths also remain shallow (<5 m) along the entire south (180°) fetch direction due to a shoal that divides Pamlico Sound (from Gull Rock to Ocracoke Inlet). At the PPP site where wave height was simulated by the model, water depth was 4.4 m (Fig. 13b). The bathymetry shows steeper slopes less than 500 m from the shore and water depths of 4 m~1 km from the shore (Fig. 13). The shallower water depths and extensive shoals around the GRG site would limit the wave growth in the model simulations, despite greater fetches at the site, resulting in the overall lower wave heights.

Fig. 13 Bathymetry. *A* The GRG site. *B* The PPP site. *C* Depth profiles at both sites. In *A*, *B*, *black circles* denote the location adjacent to each site used in the coupled hydrodynamic-wave model. *Black arrows* indicate the location of bathymetry profiles displayed. In *C*, the *asterisks* indicate the position of the model points along each profile
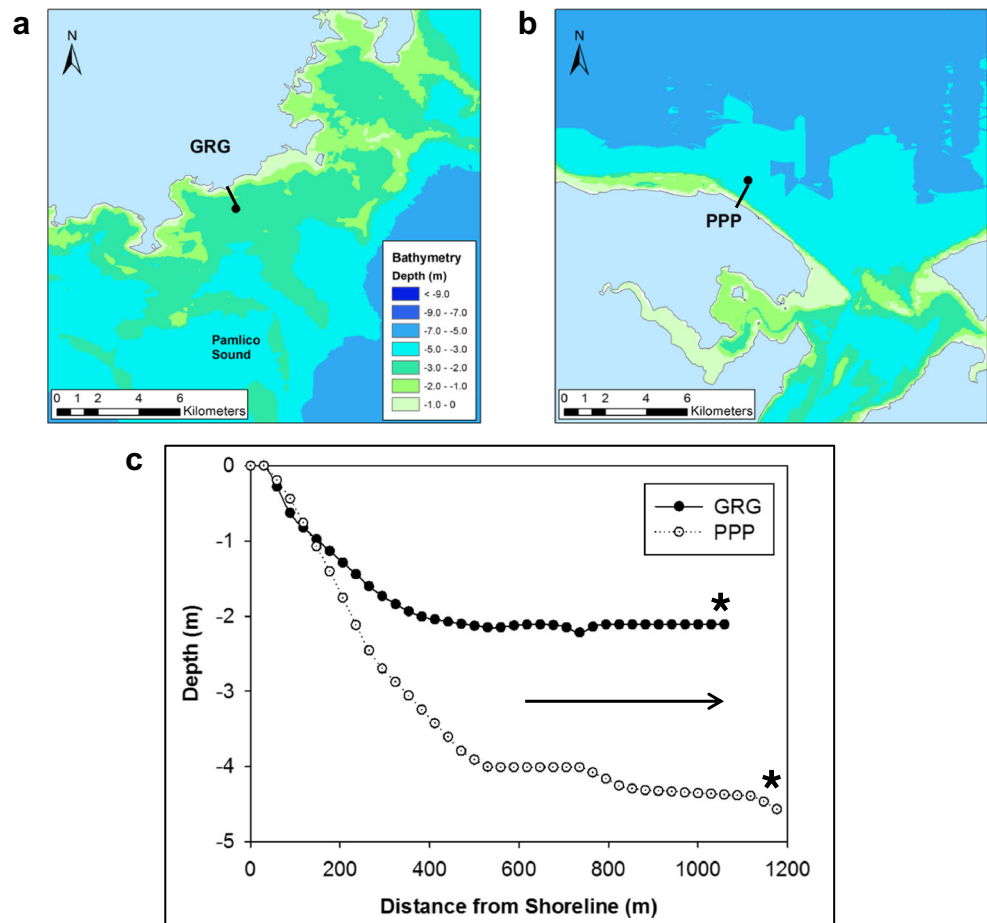
Storm Events

Wind direction, bathymetry, and resulting waves play a critical role in the amount and location of shoreline erosion. Short-duration, high-energy events can lead to significant erosion even along more resistant marsh shoreline types (i.e., GRG). While significant erosion also occurs along sediment bank shores (i.e., PPP), there is a potential for recovery post-storm, so the cumulative impact may be low over the long term. In contrast, along a marsh shoreline (i.e., GRG), the post-storm position defines a new marsh edge shoreline. This suggests that storm-driven erosion may represent a more significant contribution to the long-term rate of change along marsh shorelines than sediment bank shorelines. However, at all sites, the cumulative impact of low-frequency events such as storms was less than expected.

Coastal Management Implications

There are currently no setback requirements on the estuarine shoreline in North Carolina that are comparable to the ocean-front setbacks determined by the long-term erosion rate. There are, however, designated areas of environmental concern (AECs) that require permits for structures located within a certain distance from the shoreline and based on shoreline classification (CAMA 1974). Setbacks for structures based on rates of estuarine shoreline change could be incorporated within the existing permitting structure and would provide coastal managers with a way to manage estuarine shoreline development in the face of environmental changes such as erosion and sea-level rise. In the long-term, such policies could increase the resilience of estuarine communities and provide a regulatory mechanism for addressing shoreline retreat that does not rely on hardening the estuarine shore. However, because of the vast size of the APES, many critical locations (e.g., wetlands) are at risk, so some type of shoreline modification may be required.

Conclusions

In the micro-tidal APES system, waves have previously been identified as an important mechanism for shoreline change. Shoreline orientation and wind direction were found to be important in determining wave energy at a given site with the greatest wave heights simulated when wind direction and shoreline orientation resulted in the most exposure (greater fetch). The greatest wave heights simulated by the model occurred at the sites during the era (S2) of greatest erosion. However, no direct correlation between shoreline change rates and significant wave height was observed during the study, suggesting that this relationship is complicated by other factors such as shoreline composition and nearshore morphology

that vary between the study sites. These factors and their influence on shoreline change dynamics require further study to resolve.

The high variability observed at both fine temporal and spatial scales in comparison to the long-term historical SCRs illustrates the importance of examining shoreline change at multiple time scales and spatial resolutions. Historical rates of change provide a view of the net movement of the shoreline over decades with low methodological error. The short-term impact of recent or event-driven changes in shore position can be high, but as indicated by the spatial average shoreline position data, the cumulative impact may be lower than previously thought. The contribution of large storm events to shoreline erosion can be significant in the short term at any location but may be most important on marsh shorelines over the longer term as there is low potential for post-storm recovery of eroded material. Over short-term periods, wave energy may be a driving force behind changes in shoreline position but no direct correlation was observed in this study.

References

Ali, T.A. 2010. Analysis of shoreline-changes based on the geometric representation of the shorelines in the GIS database. *Journal of Geography and Geospatial Information Science* 1: 1–16.

Anders, F.J., and M.R. Byrnes. 1991. Accuracy of shoreline change rates as determined from maps and aerial photographs. *Shore and Beach* 59: 17–26.

Bellis, V., M.P. O'Conner, and S. R. Riggs. 1975. *Estuarine shoreline erosion in the Albemarle-Pamlico region of North Carolina*. Raleigh, North Carolina: UNC Sea Grant Publication, North Carolina State University.

Booij, N., R. Ris, and T. Aagaard. 1999. A third-generation wave model for coastal regions: 1. Model description and validation. *Journal of Geophysical Research* 104(4): 7649–7666.

Camfield, F.E., and A. Morang. 1996. Defining and interpreting shoreline change. *Ocean and Coastal Management* 32(3): 129–151.

Coastal Area Management Act [CAMA]. 1974. N.C. General Statute 113A–134.3.

Corbett, D.R., J.P. Walsh, L. Cowart, S.R. Riggs, D.V. Ames, and S.J. Culver. 2008. *Shoreline change within the Albemarle-Pamlico estuarine system*. North Carolina: East Carolina University.

Cowart, L., J.P. Walsh, and D.R. Corbett. 2010. Analyzing estuarine shoreline change: a case study of Cedar Island, North Carolina. *Journal of Coastal Research* 26: 817–830.

Cowart, L., D.R. Corbett, and J.P. Walsh. 2011. Shoreline change along sheltered coastlines: insights from the Neuse River estuary, NC, USA. *Journal of Remote Sensing* 3: 1516–1534.

Crowell, M., S.P. Leatherman, and M.K. Buckley. April 1993. Shoreline change rate analysis: long term versus short term data. *Shore and Beach*, 13–20.

Dolan, R., B. Hayden, and J. Heywood. 1978. A new photogrammetric method for determining shoreline erosion. *Coastal Engineering* 2: 21–39.

Dolan, R., H. Lins, and B. Hayden. 1988. Mid-Atlantic coastal storms. *Journal of Coastal Research* 4(3): 417–433.

Douglas, B.C., and M. Crowell. 2000. Long-term shoreline position prediction and error propagation. *Journal of Coastal Research* 16: 145–152.

Douglas, B.C., M. Crowell, and S.P. Leatherman. 1998. Considerations for shoreline position prediction. *Journal of Coastal Research* 14: 1026–1033.

Esteves, L.S., J.J. Williams, and S.R. Dillenburg. 2006. Seasonal and interannual influences on the patterns of shoreline change in Rio Grande de Sul, Southern Brazil. *Journal of Coastal Research* 22: 1076–1093.

Eulie, D.O., J.P. Walsh, and D.R. Corbett. 2013. High-resolution analysis of shoreline change and application of balloon-based aerial photography, Albemarle-Pamlico estuarine system, North Carolina, USA. *Limnology and Oceanography: Methods* 11: 151–160.

Fletcher, C.H., J.J. Rooney, M. Barbee, S.C. Lim, and B.M. Richmond. 2003. Mapping shoreline change using digital orthophotogrammetry on Maui, Hawaii. *Journal of Coastal Research, SI* 38: 106–124.

French, P.W. 2001. *Coastal defense: processes, problems and solutions*. London: Routledge.

Geis, S., and B. Bendell. 2010. *Charting the estuarine environment: a methodology spatially delineating a contiguous, estuarine shoreline of North Carolina*. Raleigh, NC: Division of Coastal Mangement.

Gentz, A.S., C.H. Fletcher, R.A. Dunn, L.N. Frazer, and J.J. Rooney. 2007. The predictive accuracy of shoreline change rate methods and alongshore beach variation on Maui, Hawaii. *Journal of Coastal Research* 23: 87–105.

Hardaway, C.S. 1980. Shoreline erosion and its relationship to the geology of the Pamlico River Estuary, North Carolina. Unpublished Masters Thesis, East Carolina University, Greenville, NC.

Jackson, N.L. and K.F. Nordstrom. 1992. Site specific controls on wind and wave processes and beach mobility on estuarine beaches in New Jersey, U.S.A. *Journal of Coastal Research* 8(1): 88–98.

Jackson, C.W., C.R. Alexander, and D.M. Bush. 2012. Application of the AMBUR R package for spatio-temporal analysis of shoreline change: Jekyll Island, Georgia, USA. *Computers and Geosciences* 41: 199–207.

Komar, P.D. 1983. Beach processes and erosion. In *CRC Handbook of coastal processes and erosion*, eds. Komar, P.D., and J.R. Moore. Boca Raton, Florida: CRC Press Inc.

Lesser, G.R., J.A. Roelvink, J.A.T.M. van Kester, and G.S. Stelling. 2004. Development and validation of a three-dimensional morphological model. *Coastal Engineering* 51: 883–915.

List, J.H., A.S. Farris, and C. Sullivan. 2006. Reversing storm hotspots on sandy beaches: spatial and temporal characteristics. *Marine Geology* 226: 261–279.

McVerry, K. 2012. *North Carolina estuarine shoreline mapping project: statewide and county statistics* (pp 1–145). North Carolina: North Carolina Division of Coastal Management.

Moore, L.J. 2000. Shoreline mapping techniques. *Journal of Coastal Research* 16: 111–124.

Mulligan, R., J.P. Walsh, and H.M. Wadman. 2015. Storm surge and surface waves in a shallow lagoonal estuary during the crossing of a hurricane. *Journal of Waterway, Port, Coastal, and Ocean Engineering* 141(4): A5014001.

NRC. 2007. *Mitigating shoreline erosion along sheltered coasts*. Washington: National Academies Press.

Pajak, M.J., and S. Leatherman. 2002. The high water line as shoreline indicator. *Journal of Coastal Research* 18(2): 329–337.

Phillips, J.D. 1986. Spatial analysis of shoreline erosion, Delaware Bay, New Jersey. *Annals of the Association of American Geographers* 76: 50–62.

Phillips, J.D. 1999. Event timing and sequence in coastal shoreline erosion: hurricanes Bertha and Fran and the Neuse Estuary. *Journal of Coastal Research* 15(3): 616–623.

Pierce, L.R. 2004. Lake waves, coarse clastic beach variability and management implications, Loch Lomond, Scotland, UK. Journal of Coastal Research 20(2): 562–585.

Riggs, S.R., and D.V. Ames. 2003. *Drowning the North Carolina coast: sea-level rise and estuarine dynamics*. North Carolina: North Carolina Sea Grant.

Roman, C.T., and K.F. Nordstrom, eds. 1996. *Estuarine shores: evolution, environments and human alterations*. London: John Wiley & Sons.

Rosen, P.S. 1980. Erosion susceptibility of the Virginia Chesapeake Bay shoreline. *Marine Geology* 34: 45–59.

Schwimmer, R.A. 2001. Rates and processes of marsh shoreline erosion in Rehoboth Bay, Delaware, U.S.A. *Journal of Coastal Research* 17: 672–683.

Stevenson, J.C., and M.S. Kearney. 1996. Shoreline dynamics on the windward and leeward shores of a large temperate estuary. In *Estuarine shores: evolution, environments and human alterations*, eds. Nordstrom, K.J., and C.T. Roman. London: John Wiley & Sons Ltd.

Stirewalt, G.L., and R.L. Ingram. 1974. *Aerial photographic study of shoreline erosion and deposition, Pamlico Sound, North Carolina*. North Carolina: North Carolina Sea Grant.

Wells, J.T., and S. Kim. 1989. Sedimentation in the Albemarle-Pamlico lagoonal system: synthesis and hypotheses. *Marine Geology* 88: 263–284.

Wilcock, P.R., Miller, D.S., Shea, R.H., and R.T. Kerkin. 1998. Frequency of effective wave activity and the recession of coastal bluffs: Calvert Cliffs, Maryland. *Journal of Coastal Research* 14(1): 256–268.

Zhang, K., B. Douglas, and S. Leatherman. 2002. Do storms cause long-term beach erosion along the U.S. east barrier coast? *The Journal of Geology* 110: 493–502.